Dispersion-shifted all-solid high index-contrast microstructured optical fiber for nonlinear applications at 1.55μm

Xian Feng*, Francesco Poletti, Angela Camerlingo, Francesca Parmigiani, Peter Horak, Periklis Petropoulos, Wei H. Loh, and David J. Richardson

Optoelectronics Research Centre, University of Southampton, Southampton, SO17 1BJ, UK
**xif@orc.soton.ac.uk*

Abstract: We report the fabrication of an all-solid highly nonlinear microstructured optical fiber. The structured preform was made by glass extrusion using two types of commercial lead silicate glasses that provide high index-contrast. Effectively single-moded guidance was observed in the fiber at 1.55μm. The effective nonlinearity and the propagation loss at this wavelength were measured to be $120W^{-1}km^{-1}$ and 0.8dB/m, respectively. Numerical simulations indicate that the fiber is dispersion-shifted with a zero-dispersion-wavelength of 1475nm and a dispersion slope of $0.16ps/nm^2/km$ respectively at 1.55μm. These predictions are consistent with the experimentally determined dispersion of + 12.5ps/nm/km at 1.55μm. Tunable and efficient four-wave-mixing based wavelength conversion was demonstrated at wavelengths around 1.55μm using a 1.5m-length of the fiber.

OCIS codes: (060.2280) Fiber design and fabrication; (060.5295) Photonic crystal fibers; (060.4370) Nonlinear optics, fibers

References and links

1. J. C. Knight, T. A. Birks, P. St. J. Russell, and D. M. Atkin, "All-silica single-mode optical fiber with photonic crystal cladding," Opt. Lett. **21**(19), 1547–1549 (1996).
   Errata, Opt. Lett. **22**, 484–485 (1997).
2. P. Russell, "Photonic crystal fibers," Science **299**(5605), 358–362 (2003).
3. T. M. Monro, Y. D. West, D. W. Hewak, N. G. R. Broderick, and D. J. Richardson, "Chalcogenide holey fibres," Electron. Lett. **36**(24), 1998–2000 (2000).
4. T. M. Monro, K. M. Kiang, J. H. Lee, K. Frampton, Z. Yusoff, R. Moore, J. Tucknott, D. W. Hewak, H. N. Rutt, and D. J. Richardson, "High nonlinearity extruded single-mode holey optical fibers," OFC2002 (OSA, Washington, DC, 2002)," Postdeadline FA1, 1–3 (2002).
5. X. Feng, A. K. Mairaj, D. W. Hewak, and T. M. Monro, "Non-silica glasses for holey fibers," J. Lightwave Technology **23**(6), 2046–2054 (2005).
6. X. Feng, T. M. Monro, P. Petropoulos, V. Finazzi, and D. Hewak, "Solid microstructured optical fiber," Opt. Express **11**(18), 2225–2230 (2003).
7. X. Feng, T. M. Monro, P. Petropoulos, V. Finazzi, and D. J. Richardson, "Extruded single-mode high-index-core one-dimensional microstructured optical fiber with high index-contrast for highly nonlinear optical devices," Appl. Phys. Lett. **87**(8), 081110 (2005).
8. S. Asimakis, P. Petropoulos, F. Poletti, J. Y. Y. Leong, R. C. Moore, K. E. Frampton, X. Feng, W. H. Loh, and D. J. Richardson, "Towards efficient and broadband four-wave-mixing using short-length dispersion tailored lead silicate holey fibers," Opt. Express **15**(2), 596–601 (2007).
9. E. Schott, -Catalogue 2000—Optical Glass, for Windows, version1.1E (Schott Glass, 2001).
10. A. Boskovic, S. V. Chernikov, J. R. Taylor, L. Gruner-Nielsen, and O. A. Levring, "Direct continuous-wave measurement of n_2 in various types of telecommunication fiber at 1.55μm," Opt. Lett. **21**(24), 1966–1968 (1996).
11. T. Hasegawa, T. Nagashima, and N. Sugimoto, "Determination of nonlinear coefficient and group-velocity-dispersion of bismuth-based high nonlinear optical fiber by four-wave-mixing," Opt. Commun. **281**(4), 782–787 (2008).
12. J. Hansryd, P. A. Andrekson, M. Westlund, J. Li, and P.-O. Hedekvist, "Fiber-based optical parametric amplifiers and their applications," IEEE J. Sel. Top. Quantum Electron. **8**(3), 506–520 (2002).
13. T. Torounidis, M. Karlsson, and P. A. Andrekson, "Fiber optical parametric amplifier pulse source: theory and experiments," J. Lightwave Technol. **23**(12), 4067–4073 (2005).

#116925 - $15.00 USD Received 8 Sep 2009; revised 15 Oct 2009; accepted 16 Oct 2009; published 21 Oct 2009

1. Introduction

Over the last few years intensive work on microstructured optical fiber (MOFs) has looked to exploit the combination of the wavelength-scale features that can be achieved in the microstructured cladding and the large index-contrasts possible between the background material and the material(s) in the microstructured regions. These features provide the opportunity for drastic tailoring of the dispersion profile of the fiber over a very broad wavelength range and allow for extremely high values of effective nonlinearity per unit length. Following pioneering work on silica MOFs [1,2], the field of high-index non-silica glass MOFs [3,4] has developed rapidly. Such fibers offer significant potential advantages over their silica counterparts, particularly in the area of highly nonlinear optical fibers, since high-index non-silica glasses, such as lead-silicate, tellurite and chalcogenide glasses, possess nonlinear indices of refraction n_2 that can be 1-3 orders of magnitude higher than that of pure silica (2.5×10^{-20} m^2/W) [5]. This should allow the implementation of compact nonlinear devices based on meter-long scale highly nonlinear MOFs fabricated using non-silica glasses. Most commonly, the low-index microstructured features in MOFs are defined by air holes (hence the term holey fibers - HFs). However, it has been found that due to the steep viscosity curve of non-silica glasses, it can be challenging to fabricate a HF with a holey cladding that conforms to a specific design and to the required tolerances. Consequently the optical properties of many fabricated non-silica glass HFs show relatively large deviations from the initial design target [5]. One of the most straightforward solutions to overcome this drawback is to use high index-contrast all-solid MOF rather than HF designs since the refractive index structure defined in the preform is accurately preserved in the fiber drawing process [6,7]. In this work, we report the fabrication of a solid one-dimensional (1D) MOF with low loss, high nonlinearity and low dispersion at 1.55μm. Tunable four-wave-mixing (FWM) based nonlinear wavelength conversion within the 1.5μm regime is then demonstrated in a 1.5m length of this MOF.

2. Fabrication

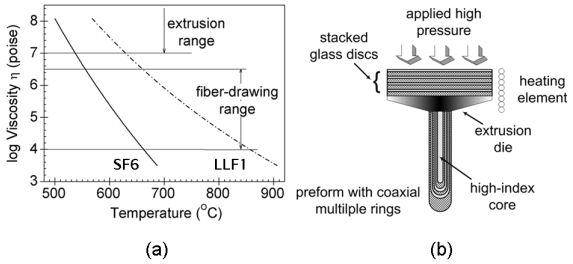

Fig. 1. (a) Viscosity curves of SF6 and LLF1 glasses; (b) schematic of forming preform with coaxial-ring structures by extrusion

Two thermally and chemically compatible commercial optical glasses, Schott SF6 and LLF1, were selected for making the solid MOF. The refractive indices of the two glasses at 1.53μm are 1.7644 and 1.5288, respectively [8]. There exists a high index-contrast of 0.2356 between these two types of glasses. As shown in the viscosity curves of these two glasses (see Fig. 1(a)), there is a thermal mismatch between the two glasses for the fabrication procedures of preform extrusion and fiber drawing, which corresponds to the viscosity ranges of 10^9-10^7 poise and $10^{6.5}$-10^4 poise respectively. However, in our fabrication attempts we found that it was possible to produce both high optical quality preforms and fibers despite this large thermal mismatch. We pursued a fiber design comprising a number of alternating high- and low-index coaxial rings, the thickness of which determines the optical properties of the fiber. The structured preform was fabricated by extruding alternately stacked high- and low-index glass discs through a circular aperture (see Fig. 1(b)). Note that all the glass discs used within our extrusion process were of high optical quality with accurately and finely polished

#116925 - $15.00 USD Received 8 Sep 2009; revised 15 Oct 2009; accepted 16 Oct 2009; published 21 Oct 2009

surfaces. The mechanism we exploit to form the multiple coaxial ring structure in the extruded preform is explained in Ref [7].

Once produced the structured preform with an outer diameter (OD) of 10mm was next elongated to cane of 1.09mm diameter and then inserted into an extruded SF6 glass jacket tube with an OD of 15.80mm and 1.10mm inner diameter (ID). Figure 2(a) shows the scanning electron microscopy (SEM) images of the MOF with 150µm OD drawn from such an assembled preform. The total yield of the fiber draw was ~100m. The fiber has a circular high-index SF6 core with a diameter of 3.7µm. Note that on the SEM photos the microstructured regions formed by the high index glass have a higher brightness than those of the low-index glass, as explained elsewhere [6]. The high-index core is surrounded by alternating LLF1 and SF6 glass rings. The three low-index rings have a thickness of 1.1, 0.6 and 0.6µm respectively. The two high-index rings have a thickness of 0.4 and 0.3µm respectively. Figure 2(b) illustrates the profile of the refractive index of the 1D MOF, according to the structural parameters obtained from the SEM image.

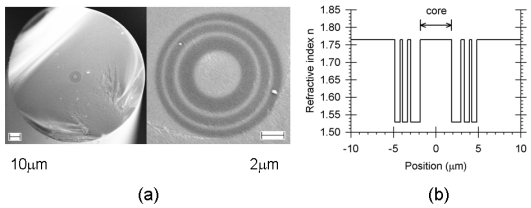

Fig. 2. (a) SEM photographs and (b) index profile of the solid MOF with 3.7µm core diameter

Figure 3 compares the structures of the 1.09mm OD cane before drawing the fiber and the central microstructure around the core in the final fiber. Four rectangular frames between the cane and the fiber are also overimposed on the images to help the eye. Note that on the original cane there was a third high-index ring which merged with the outer jacket during the fiber draw. It is obvious that the structured claddings on the cane and the fiber are completely identical in terms of geometry, even though the features that have been achieved in the final fiber are on the micron-scale. This directly illustrates the fabrication advantages of using all-solid MOFs over air-filled HFs. The former can give far more predictable and reliable control of the microstructure within the final fiber. This is obviously critically important when fabricating a MOF requiring precisely defined microstructure parameters.

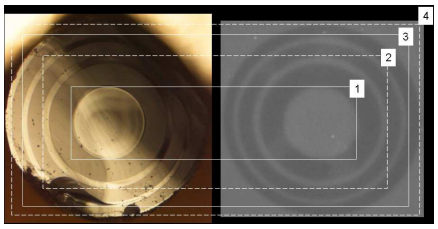

Fig. 3. Comparison between the structured cane (left) and the microstructured cladding in the final fiber (right)

3. Optical characterization of the 1D MOF

Numerical simulations of the modal properties of the fiber conducted with a full vector Finite Element Method (FEM) modal solver, often used by our group in the simulations of microstructured fibers [8], and based on the measured structure predict that this MOF supports a few higher-order modes (HOMs) at 1.55µm. Confinement loss of all HOMs is however very high and effective single-mode guidance was observed from this 1D MOF at 1.55µm in practice (see bottom row of Fig. 4(a)). Figure 4(a) also shows the simulated fundamental LP_{01} mode. Using the cutback method, the propagation loss of the fabricated solid MOF was

#116925 - $15.00 USD Received 8 Sep 2009; revised 15 Oct 2009; accepted 16 Oct 2009; published 21 Oct 2009

measured as 0.8 ± 0.2dB/m at 1.55μm (see Fig. 4(b)). The total cutback length used was 2.4m. This loss figure is very close to the bulk attenuation deduced from the published data of commercial Schott SF6 glass [9], and is also one of the lowest reported loss values so far for a non-silica glass MOF to the best of our knowledge. We attribute the excellent loss to the following: (1) the starting discs used for preform extrusion were finely polished to ensure a high optical quality and (2) the extrusion was optimized in terms of temperature and speed to minimize the formation of any defects in the structured preform. This is in contrast to the conventional soft-glass HF fabrication procedures which involve either extrusion [4] or drilling [5,6], which tend to produce significant surface roughness and/or surface defects in the original preforms that impact the interface quality in the final fibers and can give rise to relatively high attenuation due to light scattering at the interfaces between the glass and the air-filled holes.

The effective nonlinearity γ of the 1D MOF was measured as $120W^{-1}km^{-1}$ at 1.55μm using the Boskovic method [10]. This is ~120 times higher than that of a standard single-mode silica optical fiber (SMF28). From the numerical modeling, the effective mode area A_{eff} of the 1D MOF was calculated to be $6.7\mu m^2$ at 1.55μm. Using the values of the nonlinear refractive indices n_2 of the two glasses, the effective nonlinearity γ of the 1D MOF was calculated to be $130W^{-1}km^{-1}$ at 1.55μm, which agrees well with the measured value.

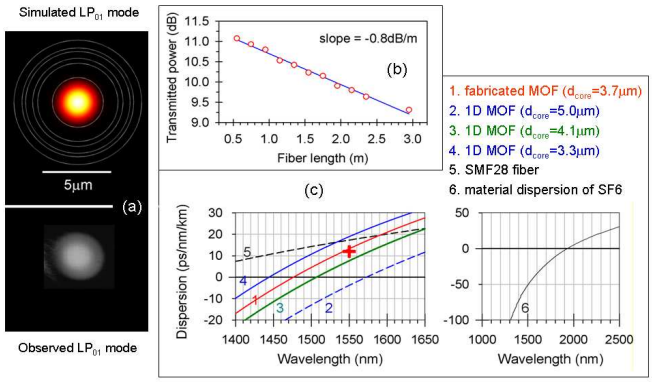

Fig. 4. (a) Simulated (upper) and observed (lower) LP_{01} mode of 1D MOF; (b) linear fitting of the transmitted power (on a log scale) from the output end of 1D MOF, using the cutback method; (c) calculated dispersion curve and measured dispersion (red cross point at 1.55μm) of 1D MOF with core diameter (d_{core}) of 3.7μm, the dispersion curves of 1D MOF with core diameter of 5.0, 4.1 and 3.3μm, silica SMF28 fiber, and bulk SF6.

Using the FWM method [11], the dispersion of the 1D MOF at 1.55μm was measured to be + 12.5ps/nm/km (see the marked cross symbol in Fig. 4(c)). Using the SEM photo of the fiber (see Fig. 2(a)), the dispersion curve of the fabricated 1D MOF was numerically calculated (see Fig. 4(c), using the FEM and independently confirmed by a semi-analytic transfer matrix approach. The plot indicates that this 1D MOF is in practice a dispersion-shifted fiber with a zero-dispersion-wavelength (ZDW) of 1475nm and a dispersion slope $0.16ps/nm^2/km$ at 1.55μm, respectively. This is in good agreement with the measurement. For reference, the dispersion curve of the commercial silica fiber SMF28 is also illustrated in Fig. 4(c). At 1.55μm the dispersion values of the MOF and silica SMF28 are very close, even though the effective nonlinearity of the MOF is 120 times higher than that of SMF28. A few meters of this 1D MOF can therefore exhibit a total nonlinearity equal to that of several hundreds of meters of SMF28 whilst exhibiting much less net dispersion – an important property for many nonlinear applications such as FWM. Figure 4(c) also illustrates the material dispersion of the bulk SF6 glass, the calculated dispersion curves of the 1D MOFs with the core diameter of 5.0μm, 4.1μm and 3.3μm using the same structured cane as the fabricated MOF. It can be seen that when reducing the geometrical dimensions, the wavelength-scale feature in the microstructured cladding generates strong waveguide

#116925 - $15.00 USD Received 8 Sep 2009; revised 15 Oct 2009; accepted 16 Oct 2009; published 21 Oct 2009

dispersion opposite in sign to the material dispersion of the core glass and then shifts the ZDW of the fiber to shorter wavelengths. The ZDW of the fiber shifts from 1.57μm to 1.44μm when the core diameter of the 1D MOF is scaled down from 5.0μm to 3.3μm.

4. Experimental demonstration of four-wave mixing

One of the most important applications of a dispersion-tailored highly nonlinear fiber is for FWM-based nonlinear wavelength conversion. By combining a strong pump wave at angular frequency (ω_p) with a signal at another frequency (ω_s) in a highly nonlinear fiber, parametric gain can be achieved [12]. At the same time, a converted idler (ω_i) will be generated at the frequency $\omega_i = 2\omega_p - \omega_s$. In order to obtain efficient and broadband FWM, a highly nonlinear fiber with a low dispersion, a low dispersion slope, and a short propagation length is required. For broadband FWM, phase matching conditions cannot be satisfied simultaneously at all wavelengths and thus the propagation distances are limited by the phase mismatch, that is, by the fiber dispersion. Nonlinear gain thus has to be sufficiently large over this limited distance, irrespective of the linear losses, which are only relevant over much longer lengths of the fiber. Here we use the product of γL_{eff}, where L_{eff} is the effective length of the fiber ($L_{eff} = [1-\exp(-\alpha*L)]/\alpha$; L: the fiber length; α: the fiber attenuation.) as the figure of merit to evaluate the nonlinear gain. The fabricate all-solid MOF provides a FOM of two orders of magnitude greater than the standard SMF28 fiber. Thus this 1D MOF is a suitable nonlinear medium for effective FWM at telecommunications wavelengths. Figure 5 illustrates the experimental setup for the demonstration of FWM-based wavelength conversion in this solid MOF. The pump wave was derived from a 10GHz mode-locked laser, which generated ~7ps full-width-half-maximum (FWHM) pulses at 1545.5nm. The pulses were amplitude modulated according to a 2^{31}-1 pseudorandom bit sequence (PRBS) using a lithium-niobate ($LiNbO_3$) Mach-Zehnder modulator (MOD) and then amplified using a high power erbium-doped fiber amplifier (HP-EDFA). A bandpass filter (BPF) was employed to remove any undesired amplified spontaneous emission (ASE) noise resulting from the EDFA. A separate amplified and filtered CW signal generated from a tunable laser source operating across the C-band was used as the probe signal. Polarization controllers (PCs) were used to control the state of polarization of the two beams and to align them to the polarization axis of the 1D MOF. The pulsed pump was combined with the CW signal in a 90/10 coupler. The combined beam was free-space launched into a 1.5m length of MOF with a coupling efficiency of ~35%. Therefore, the average powers of the pump and the signal launched into the fiber were 24.5dBm and 3dBm respectively.

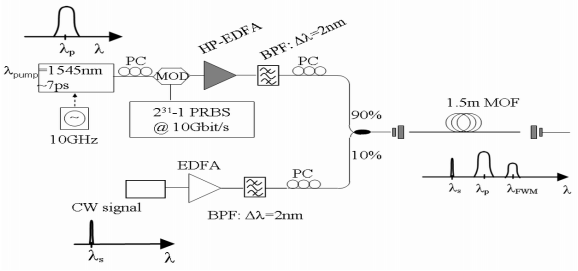

Fig. 5. Experimental setup of FWM-based wavelength conversion of a short-pulse source.

Figure 6(a) shows the measured spectral traces at the output of the fiber when the CW signal wave was tuned from 1542nm to 1530nm. The low loss, low dispersion and high nonlinearity per unit length of the MOF used in this experiment have allowed us to observe parametric wavelength conversion of the pump pulse over a wide range of wavelengths that span the upper part of the C-band, despite the pump wavelength sitting far away from the ZDW of the fiber. As illustrated in Fig. 6(b), the power conversion efficiency of FWM (η_{FWM}) here is defined as the ratio of the peak power of the converted pulsed idler wave (P_{idler}) to the pulsed pump power (P_{pump}) i.e., $\eta_{FWM} = P_{idler}-P_{pump}$ (on a dB scale). Figure 6(c) shows that the

#116925 - $15.00 USD Received 8 Sep 2009; revised 15 Oct 2009; accepted 16 Oct 2009; published 21 Oct 2009

experimental −3dB wavelength-conversion bandwidth is ~16nm and the maximum η_{FWM} is −41.5dB. The performance of the system was also studied numerically. Figure 6(c) gives the calculated η_{FWM} with various fiber lengths ranging from 1.5m to 6.0m. As can be seen, different sets of −3dB-bandwidth and maximum conversion efficiency exist for different fiber lengths. For example, the −3dB-bandwidth of η_{FWM} is ~11nm with a maximum η_{FWM} of −33dB when using a 6m-length of MOF, while a −3dB-bandwidth of ~17nm and a maximum η_{FWM} of −40dB can be achieved using a fiber length of 1.5m, which agrees very well with the experimental result. It is expected that both 3dB-bandwidth and maximum η_{FWM} can be largely increased if the fiber nonlinearity can be further enhanced and the dispersion and dispersion slope can be tailored down to near zero at 1.55μm.

In addition, we have measured the autocorrelation traces of the input pump and the output idler pulses, which were carefully filtered (care was taken to avoid any undesired filtering of the idler spectrum itself). We observed a reduction in pulse duration from 7ps at the input to 4.8ps at the output of the system (see Fig. 6(d)) and the corresponding explanation can be seen in Ref [13]. This compression factor was also predicted by our numerical simulations of the wavelength conversion scheme.

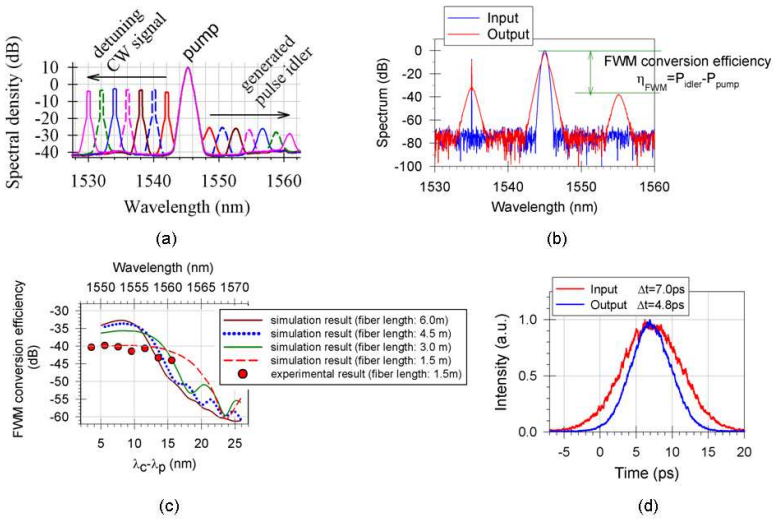

Fig. 6. (a) Measured spectral traces of FWM-based wavelength conversion in the 1.5m-length of MOF using a pulsed pump and tunable CW signal source; (b) illustration of the definition of FWM conversion efficiency with pulsed pump; (c) calculated curves of the FWM conversion efficiency using different fiber length under the experimental conditions (Note that the pulsed pump wavelength is fixed at 1545.5nm as well as its power.); (d) observed autocorrection traces of the input pump and the output idler pulses.

5. Conclusions

In conclusion, we report the fabrication of an all-solid high index-contrast 1D microstructured optical fiber using an extrusion technique. The MOF combines high nonlinearity, a low dispersion value at 1.55μm, and one of the lowest ever reported losses for non-silica glass highly nonlinear MOFs. Under a pulse-pumping scheme, tunable FWM-based wavelength-conversion was demonstrated within the C band using just a 1.5m length of MOF. Tunable wavelength conversion over ~17nm operating window (−3dB-bandwidth) and the maximum conversion efficiency of −40dB was obtained. Our results illustrate the potential to develop efficient FWM-based nonlinear parametric devices based on short lengths of all-solid non-silica MOFs.

#116925 - $15.00 USD Received 8 Sep 2009; revised 15 Oct 2009; accepted 16 Oct 2009; published 21 Oct 2009

Acknowledgement

The research leading to these results has received funding in part from the Engineering and Physics Science Research Council (UK) and the European Communities Seventh Framework FP/2007-2013 under grant agreement 224547.

#116925 - $15.00 USD Received 8 Sep 2009; revised 15 Oct 2009; accepted 16 Oct 2009; published 21 Oct 2009